Available online at www.sciencedirect.com
ScienceDirect
Pattern Recognition Letters 29 (2008) 1236–1244
Pattern Recognition Letters
www.elsevier.com/locate/patrec

A new normalized method on line-based homography estimation

Hui Zeng *, Xiaoming Deng, Zhanyi Hu

National Laboratory of Pattern Recognition (NLPR), Institute of Automation, Chinese Academy of Sciences, P.O. Box 2728, Beijing 100080, PR China

Received 4 April 2007; received in revised form 4 January 2008
Available online 20 February 2008

Communicated by P. Bhattacharya

Abstract

It is a conventional belief that line-based approaches perform better than point-based ones for homography estimation, as the line-fitting is generally more noise resistant than point detection. In this note, we show that blithely using line-based estimation is a risky business. More specifically, we show that when the image line(s) is (are) passing through or close to the origin, the line-based homography estimation could become wildly unstable whereas the point-based estimation performs normally. To tackle this problem, a new normalized method specially designed for line-based homography estimation is proposed and validated by extensive experiments.

Keywords: Point-based homography estimation; Line-based homography estimation; Visual metrology; Data normalization

1. Introduction

Homography played an important role in visual metrology (Criminisi et al., 1999; Criminisi, 2001; Wang et al., 2004), camera calibration (Zhang, 2000; Triggs, 1998) and 3D reconstruction (Wang et al., 2005; Wright et al., 2006). There are many kinds of methods for homography estimation, where the direct linear transformation (DLT) (Abdel-Aziz and Karara, 1971) is the most practical and convenient one due to its linearity and simplicity. Under the DLT paradigm, either point correspondences or line correspondences could be used, and in theory the line-based estimation and the point-based estimation is equivalent. It is widely believed, and in most cases, it is indeed true, that the line-based estimation is better than the point-based one in terms of noise resistance from the computational point of view. However, we found that the performance of the line-based homography estimation is dependent on the chosen image coordinate system. If by chance an image line is passing through or close to the origin of the chosen image coordinate system, the line-based estimation will become wildly unstable whereas the point-based estimation still performs normally. This indicates that there exist some specialties in line-based estimation from numerical point of view although the underlying theory is the same with the point-based one.

In his famous normalized 8-point algorithm for the fundamental matrix estimation, Hartley proposed a pre-data normalization step to improve the conditioning of the coefficient matrix (Hartley, 1997). Hartley's data normalization approach is specifically designed for point coordinates, a direct copy of it for line-based homography estimation seems inappropriate as the third coordinate of an image line could be zero, whereas the third coordinate of an image point in the homogenous coordinates is always equal to 1. Based on this, we also introduce a normalization scheme for line coordinates in this work, and the scheme is shown effective from extensive experiments.

Of course, if many line correspondences are available in practical applications, one or a few image lines close to the origin is evidently not too serious for the estimation. Here our work is particularly for those applications where the number of line correspondences is not large due to either the practical concern or the task imposition. For example,

* Corresponding author. Tel.: +86 10 62542946; fax: +86 10 62551993.
E-mail address: hzeng@nlpr.ia.ac.cn (H. Zeng).

0167-8655/$ - see front matter © 2008 Elsevier B.V. All rights reserved.
doi:10.1016/j.patrec.2008.01.031

for visual metrology, the template cannot be too complicated. In our case, our "⊡"-type template contains only 4 pairs of parallel lines, one image line close to the origin can bring forth gross estimation errors.

The rest of the paper is organized as follows. In Section 2, some preliminaries about homography, line-based homography estimation and the condition number of the measurement matrix are introduced. Then a new normalized method for line-based homography estimation is presented in Section 3. Section 4 reports the experimental results and some concluding remarks are listed in Section 5.

2. Preliminaries

2.1. Plane-to-image homography

In this work, an image point is denoted by $\tilde{\mathbf{m}} = (u, v, 1)^{\mathrm{T}}$ in the homogenous coordinates and a point on space plane by $\widetilde{\mathbf{M}}_{\pi} = (X, Y, 1)^{\mathrm{T}}$. Then the mapping between a point on the space plane to its image is a 2D projective transformation, called plane-to-image homography, expressed as

$$s\begin{bmatrix} u \\ v \\ 1 \end{bmatrix} = \begin{bmatrix} h_{11} & h_{12} & h_{13} \\ h_{21} & h_{22} & h_{23} \\ h_{31} & h_{32} & h_{33} \end{bmatrix}\begin{bmatrix} X \\ Y \\ 1 \end{bmatrix} \tag{1}$$

or

$$s\tilde{\mathbf{m}} = \mathbf{H}\widetilde{\mathbf{M}}_{\pi} \tag{2}$$

Usually, $\mathbf{H}$ is a non-singular 3×3 homogenous matrix with 8 degrees of freedom as it can only be defined meaningfully up to a scale factor. The homography can be uniquely determined from four correspondences from space points (no three points are collinear) to image ones.

Let $\mathbf{L}$ be a line on the space plane and $\mathbf{l}$ its corresponding image line. From the duality principle about points and lines as shown in (Hartley and Zisserman, 2003), the line mapping can be expressed as

$$s\mathbf{L} = \mathbf{H}^{\mathrm{T}}\mathbf{l} \tag{3}$$

Similarly 4 line correspondences can be used to determine the homography $\mathbf{H}$. Once $\mathbf{H}$ is obtained, an image point can be back-projected to the world plane via $\mathbf{H}^{-1}$, so the distances of points on the world plane can be measured.

2.2. Line-based homography estimation under the DLT paradigm

Estimation by the DLT is meant to get some linear constraints on homography $\mathbf{H}$ via Eq. (3) from some line correspondences, and then use them to estimate $\mathbf{H}$ by minimizing the total sum of algebraic errors as shown below, see also Faugeras (1993), Hartley and Zisserman (2003)) for more details.

Let $\mathbf{L}_i = (A_i, B_i, C_i)^{\mathrm{T}} \leftrightarrow \mathbf{l}_i = (a_i, b_i, c_i)^{\mathrm{T}} (1 \leqslant i \leqslant n)$ be a pair of line correspondences, then 3 linear constraints in the entries of $\mathbf{H}$ can be obtained as

$$\mathbf{U}_i\mathbf{h} = \begin{bmatrix} 0^{\mathrm{T}} & -C_i\mathbf{l}_i^{\mathrm{T}} & B_i\mathbf{l}_i^{\mathrm{T}} \\ C_i\mathbf{l}_i^{\mathrm{T}} & 0^{\mathrm{T}} & -A_i\mathbf{l}_i^{\mathrm{T}} \\ -B_i\mathbf{l}_i^{\mathrm{T}} & A_i\mathbf{l}_i^{\mathrm{T}} & 0^{\mathrm{T}} \end{bmatrix}, \quad \mathbf{h} = 0,\ i = 1, 2, \ldots, n \tag{4}$$

where $\mathbf{h} = [h_{11}, h_{21}, h_{31}, h_{12}, h_{22}, h_{32}, h_{13}, h_{23}, h_{33}]^{\mathrm{T}}$. Although there are three constraints in Eq. (4), only two of them are linearly independent. In practice, usually all the three constraints are used to gain robustness (Agarwal et al., 2005; Kanatani and Ohta, 1999). For all the n line correspondences, the measurement matrix can be written as

$$\mathbf{U} = (\mathbf{U}_1^{\mathrm{T}}, \mathbf{U}_2^{\mathrm{T}}, \ldots, \mathbf{U}_n^{\mathrm{T}})^{\mathrm{T}} \tag{5}$$

Then the least-squares solution for $\mathbf{h}$ is the singular vector corresponding to the smallest singular value of $\mathbf{U}$.

2.3. The condition number of the measurement matrix

The condition number of the measurement matrix is an important factor in the analysis of the stability of linear problems (Horn and Johnson, 1990). If the singular values of the measurement matrix $\mathbf{U}$ are $d_1, d_2, \ldots, d_9 (d_1 \geqslant d_2 \geqslant \cdots \geqslant d_9)$, then the condition number of the matrix $\mathbf{U}$ is defined as

$$\lambda = d_1/d_8 \tag{6}$$

It is generally observed that if the measurement data are noise-free, the larger the condition number of the measurement matrix is, the more sensitive to noise the method is. In his famous work (Hartley, 1997), Hartley showed that the main reason for the poor conditioning of the measurement matrix is lack of homogeneity in the data coordinates. By pre-normalizing the image coordinates to reduce the condition number, the estimation robustness can be substantially increased.

3. A new normalized method for line-based homography estimation

3.1. A case of instability

In our application on visual metrology, we find that for a given quadruplet of line correspondences, if one or more image lines are passing through or close to the origin, the homography estimation by the DLT becomes wildly unstable, and at this time, the condition number of the measurement matrix is very large too. We think this instability is chiefly due to the ill-conditioning of the measurement matrix. Here is a theoretical analysis:

In our work, an image line is defined under the normal parametrization as $\sin\theta \cdot u - \cos\theta \cdot v + \rho = 0$, where θ is the including angle between the line and the positive u-axis, ρ is the distance of the line from the origin. Let the coordinates of a line be $\mathbf{l}_i = (a_i, b_i, c_i)^{\mathrm{T}}$, thus $a_i^2 + b_i^2 = 1, \rho \geqslant 0$. When a line passes through the origin, its third coordinate $c_i = 0$. In this case, Hartley's normalization method for

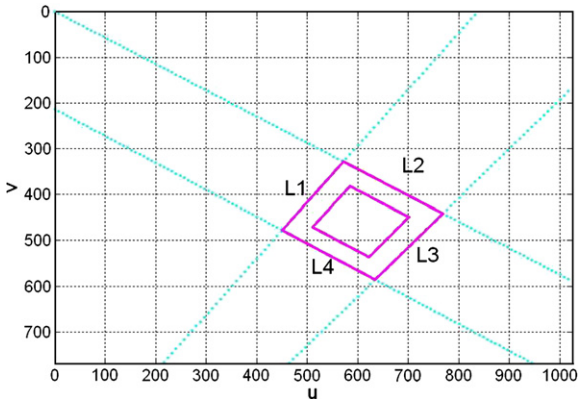

Fig. 1. The simulated image of the reference template.

image point coordinates is longer usable. Although Hartley also considered the case of normalizing points at (or near) infinity, he did not elaborate on it. We should find a new normalization method for line coordinates.

When there exist one or more image lines passing through or close to the origin, if we keep $a_i^2 + b_i^2 = 1$, the variety of the third coordinate c_i generally much larger than a_i and b_i. Then according to Hartley's reasoning, the condition number of the corresponding measurement matrix will be large. On the other hand, if we set $a_i^2 + b_i^2 + c_i^2 = 1$, the situation cannot be improved much, the condition number of the measurement matrix is still too large. Here is a specific example.

As shown in Fig. 1, the quadrilateral is the projected image of our simulated "▣"-type reference template for visual metrology, the origin of the image coordinate system is at the upper-left corner. The distance from the origin to the line L_2 is much smaller (close to 0) than those of other 3 lines. In order to investigate the relative space distribution of the four labeled lines, we define that the coordinates' Frobenius norm of the lines in Fig. 2 is 1. As shown in Fig. 2a, since $c_2 \ll c_i$ $(i = 1, 3, 4)$, and the corresponding point of the line L_2 in the (a, b, c) parameter space is far separated from those of other lines. Moreover, the corresponding points of the other three lines are much congregated. Then according to Hartley's theory, the problem is bad conditioned and the estimation will be sensitive to noise.

3.2. A new normalization

Inspired by Hartley's point-based normalization approach, we present a new normalization approach specially designed for line coordinates (Hartley, 1997). Similarly, a simple transformation is performed before formulating the linear equations, and then the condition number of the measurement matrix is improved. Our experimental results show that the normalization could lead to a substantial increase in the stability of the line-based homography estimation.

Based on the above analysis, here is our new normalization for line-based estimation:

Given a set of image lines $\mathbf{l}_i = (a_i, b_i, c_i)^{\mathrm{T}}$ $(i = 1, 2, 3, \ldots, n)$, set $t_1 = \sum_{i=1}^{n} a_i, t_2 = \sum_{i=1}^{n} b_i, t_3 = \sum_{i=1}^{n} c_i$. Construct the transformation $\mathbf{T}_1$ as follows:

$$\mathbf{T}_1 = \begin{bmatrix} 1 & 0 & -t_1/t_3 \\ 0 & 1 & -t_2/t_3 \\ 0 & 0 & 1 \end{bmatrix} \tag{7}$$

Then after the transformation of $\mathbf{l}'_i = \mathbf{T}_1 \cdot \mathbf{l}_i$, the transformed line coordinates $\mathbf{l}'_i = (a'_i, b'_i, c'_i)^{\mathrm{T}}$ satisfy $\sum_{i=1}^{n} a'_i = 0$ and $\sum_{i=1}^{n} b'_i = 0$. Here the centroid of the transformed line coordinates lies on the c-axis. That is to say, the transformation $\mathbf{T}_1$ makes the relative distribution of the line coordinates more homogenous about the c-axis in the $O - abc$ coordinate system.

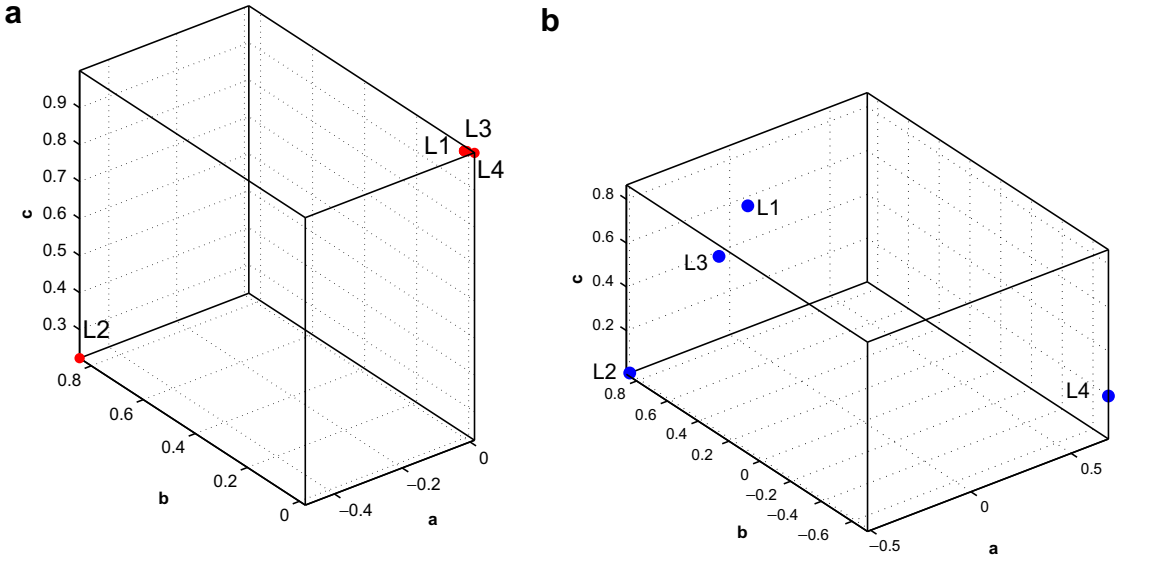

Fig. 2. The relative space distribution of the line.

Let $s = \left[\frac{\sum_{i=1}^{n}(a_i'^2+b_i'^2)}{2\cdot\sum_{i=1}^{n}c_i'^2}\right]^{1/2}$, and construct the transformation $\mathbf{T}_2$ as

$$\mathbf{T}_2 = \begin{bmatrix} 1 & 0 & 0 \\ 0 & 1 & 0 \\ 0 & 0 & s \end{bmatrix} \tag{8}$$

Now, let us have a note on the "worst" scenario. If all $c_i' = 0$, all lines are passing through the origin and $s \to \infty$. From the principle of projective geometry, we can see that this is a degenerate configuration and we cannot determine a unique homography from such line correspondences. In our work, we use a "⊡"-type reference template, this dangerous case is impossible to arise.

Then after the transformation of $\mathbf{l}_i'' = \mathbf{T}_2 \cdot \mathbf{l}_i'$, the line coordinates $\mathbf{l}_i'' = (a_i'', b_i'', c_i'')^{\mathrm{T}}$ satisfy $\sum_{i=1}^{n}(a_i''^2 + b_i''^2) = 2\sum_{i=1}^{n}c_i''^2$. Let the root mean square distance from the transformed line coordinates to plane Oab be d_1 and let the root mean square distance to c-axis be d_2, then the ratio of d_1 to d_2 is $\sqrt{2}$. This makes the relative distribution of the line coordinates more homogenous in the abc space.

Finally, set $\mathbf{l}_i''' = \mathbf{l}_i''/\|\mathbf{l}_i''\|$, then the transformed line coordinates lie on the sphere centered at the origin and of radius 1.

After the above normalization, the relative distribution of the four simulated image lines is shown in Fig. 2b. We can see that our proposed normalization can improve the homogeneity of the line coordinates distribution, hence an improvement in the stability of the estimation.

Here is a summary of our normalization steps:

Given $n \geqslant 4$ space to image line correspondences $\{\mathbf{L}_i \leftrightarrow \mathbf{l}_i\}$.

(1) Construct two transformations $\mathbf{T}_1$ and $\mathbf{T}_2$ to normalize the image lines using Eqs. (7) and (8).
(2) Construct two transformations $\mathbf{T}_1'$ and $\mathbf{T}_2'$ to normalize the space lines in the same way.
(3) Transform the line coordinates using $\mathbf{l}_i'' = \mathbf{T}_2\mathbf{T}_1 \cdot \mathbf{l}_i$ and $\mathbf{L}_i'' = \mathbf{T}_2'\mathbf{T}_1' \cdot \mathbf{L}_i$, and set their Frobenius norms equal to 1. Thus we can obtain a set of new line correspondences $\{\mathbf{L}_i'' \leftrightarrow \mathbf{l}_i''\}$ and use the DLT method to estimate the homography $\mathbf{H}'$.
(4) Denormalization. The homography for the original coordinates is obtained as $\mathbf{H} = \mathbf{T}_1^{\mathrm{T}}\mathbf{T}_2^{\mathrm{T}}\mathbf{H}'\mathbf{T}_1'^{-\mathrm{T}}\mathbf{T}_2'^{-\mathrm{T}}$.

4. Experiments

4.1. Experiments with simulated data

The simulation experiments aim at testing the robustness and accuracy of our normalized method, and comparing it with the DLT method. In order to ensure the comparability of the two methods, all tests are taken under the same camera parameters and simulation data. During the simulations, the camera's setup is: $f_u = 1200$, $f_v = 1000$, $\alpha = 0.1$, $u_0 = 512$, $v_0 = 384$. The image resolution is of 1024×768 pixels. The camera extrinsic parameters are: rotation axis $\mathbf{r} = (2,1,4)^{\mathrm{T}}$, translation $\mathbf{T} = (20, 20, 260)^{\mathrm{T}}$ and the rotation angle is set respectively in each test.

For both methods, we generate a "⊡"-type reference template, and equidistantly select 100 points on each side of the template. The 100 image points on each side are fitted to a line via a least-squares algorithm. Then the homography between the reference plane and the image plane can be estimated and an image point can be mapped to the Euclidean space. At last, the distance between two space points can be determined. In order to provide more statistically meaningful results, for each test, we randomly select 100 pairs of space points and use their corresponding image points to estimate their distances. Define the relative measurement error as

$$E_{\mathrm{rela}} = \left(\frac{|D_{\mathrm{t}} - D_{\mathrm{e}}|}{D_{\mathrm{t}}} \times 100\right)\% \tag{9}$$

where D_{t} is the true distance, D_{e} is the estimated distance. In each test, we use the averaged absolute error and the averaged relative error of the 100 computed distances as the final results.

At first, we test the robustness of the new normalized method by comparing the condition number of the two methods without adding image noise in the simulated data. As described in Section 2.3, the smaller the condition number of the measurement matrix is, the more robust the method is. For each simulation, we randomly select a rotation angle in $[-100°, 100°]$. About 100 independent trials are done and the results are shown in Fig. 3. We can see that the condition number of the DLT method is always larger than that of our normalized method. That is to say, our normalized method is always more robust than the DLT method.

Secondly, we investigate the influences of the camera rotation angle on the two methods. Gaussian noise with mean 0 and standard deviation 1.5 is added to the coordinates of the simulated image points. We vary the rotation angle α from $-100°$ to $100°$. For each angle, we repeat

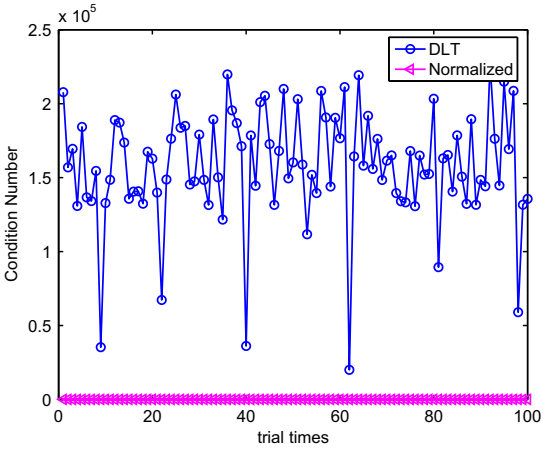

Fig. 3. A comparison of the condition number of the two method.

100 times and calculate the absolute measurement error, the mean and the variance of the condition number. The averaged results of the absolute measurement errors are shown in Fig. 4a, and the mean and the variance of the condition number are shown in Fig. 4b and c. We can see that for the DLT method, some gross estimation errors appear under some special camera poses, and the variance of the corresponding condition number is large. From the distribution of the image lines we can find that, for these camera poses with larger measurement errors, there always exist one or more image lines passing through or close to the origin of the image coordinate system. Fig. 1 is the simulated image of the reference template with $\alpha = 39°$. From Fig. 4 we can see that this rotation angle falls in the band of the angles that manifest large errors.

Then, we investigate the influences of the image noise level on the two methods. Gaussian noise with mean 0 and standard deviation ranging from 0 to 5 pixels is added to the coordinates of the image points. At each noise level, 100 runs are done. Figs. 5a and b are the results of the absolute measurement error and the relative measurement error. Figs. 5c and d are the results of the mean and the variance of the condition number. We can see that both the absolute errors and the relative errors increase roughly linearly with the noise level. The results of our normalized method are always better than those by the DLT method. When the noise level of the simulated data is not zero, the condition number' s mean and the variance of the DLT method are always larger than those of our normalized method. Hence when there is noise present in the image, our normalized method is more noise resistant than the DLT method.

Finally, we investigate whether by simply translating the origin to somewhere that no line is close to it could handle the issue. The root cause of the unstability is partly due to the choice of the image system. An apparent way to solve the problem is to fix the center of the image quadrilateral as the origin of the image system, as shown in Fig. 6. So we first compute the image points of the reference template under the translated image system. Then we do the homography estimation using the DLT method. Finally the distance between two space points can be calculated by the estimated homography and their corresponding translated image coordinates. We name such a procedure as "Trans-DLT" method, and compare it with our normalized method under different camera rotation angles. Gaussian

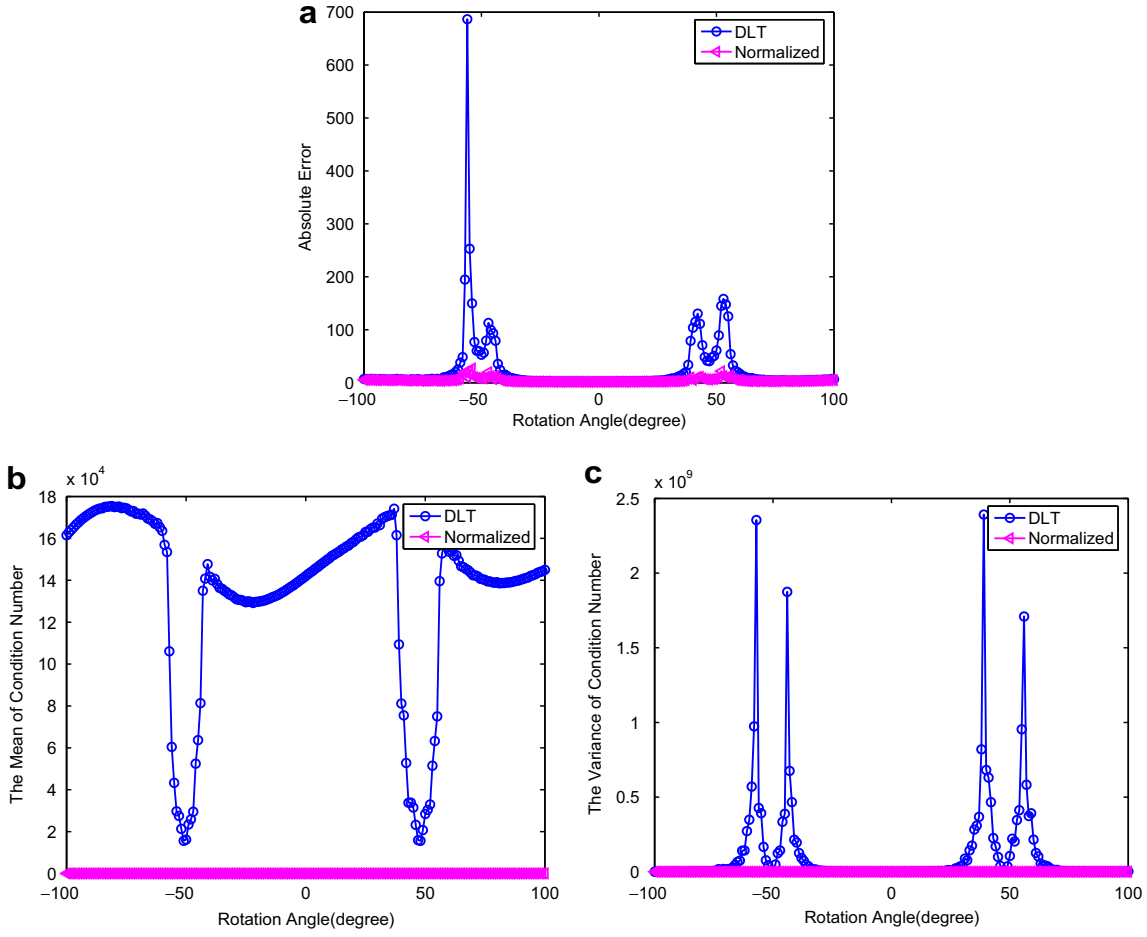

Fig. 4. A comparison of the absolute measurement error, the condition number's mean and variance of the two methods (a) the absolute measurement error (b) the mean of the condition number (c) the variance of the condition number.

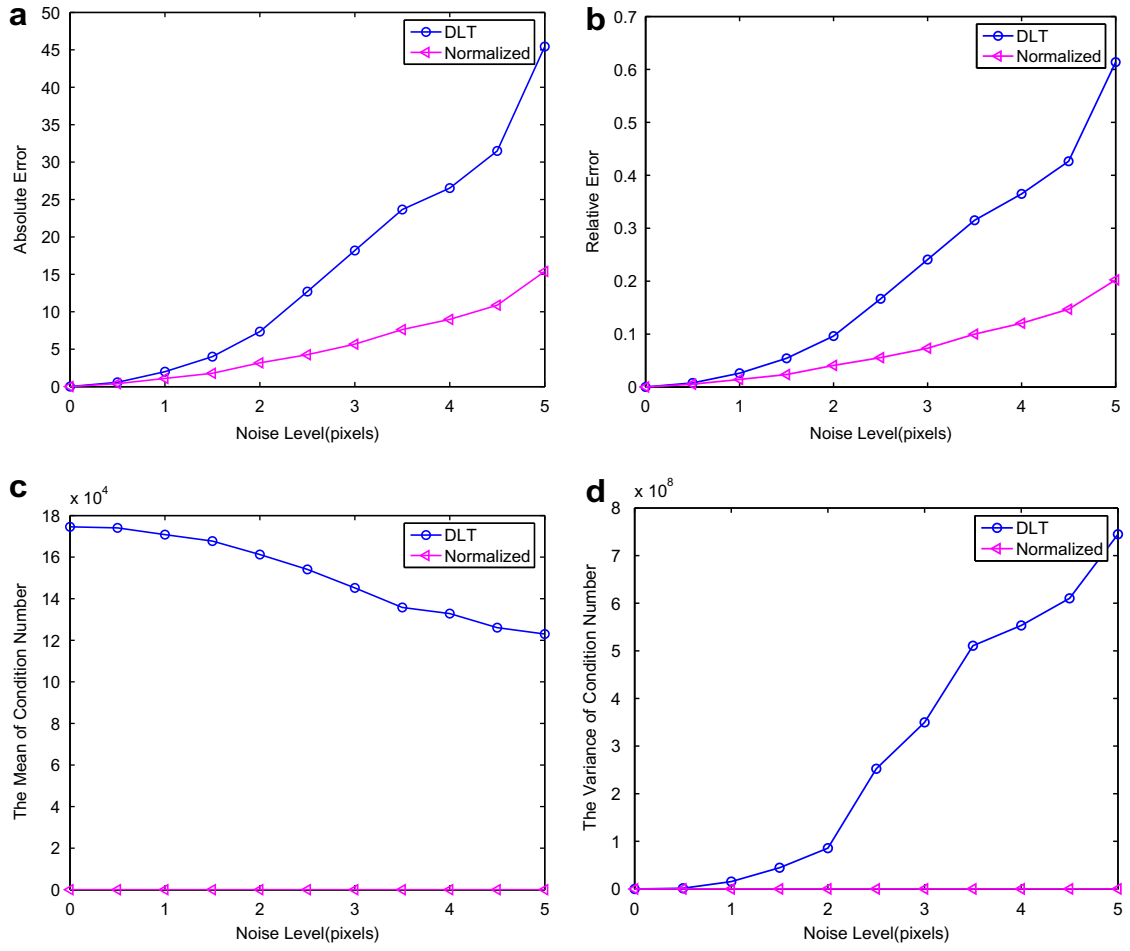

Fig. 5. A comparison of the measurement's absolute error and relative error, the condition number's mean and variance of the two methods.

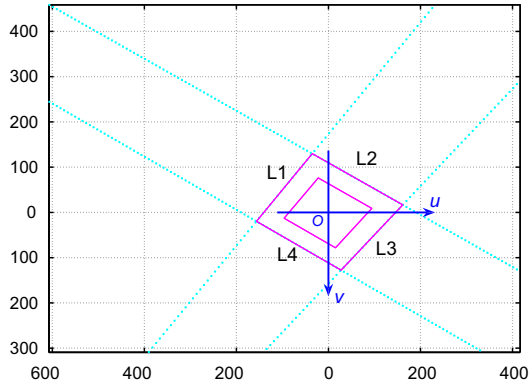

Fig. 6. The simulated image under the translated image system.

noise with mean 0 and standard deviation 1.5 is added to the simulated image points. For each angle, we repeat 100 times and the averaged results are shown in Fig. 7. We can see that for the "TransDLT" method, the mean and the variance of the condition number is larger under some camera poses, and the corresponding estimation errors are larger too. In Comparison with Fig. 4, we can conclude that the "TransDLT" method is better than the DLT method, but it is not so good as our normalized method. Although the simple translation can improve the distribution of the data coordinates, it cannot achieve the similar stability of the "normalized" method. From Fig. 7b and c, we can see that the simple translation cannot change the ill conditioning of the problem thoroughly.

A line can be parameterized with different forms and the normalization on different line parameterizations seems differ. So we carry out the experiments on two popular line parameterizations. For line $\mathbf{l}_i = (a_i, b_i, c_i)^{\mathrm{T}}$, the "DLT" and "Normalized" methods use the constraint $a_i^2 + b_i^2 = 1$, and the "DLT2" and "Normalized2" methods use the constraint $a_i^2 + b_i^2 + c_i^2 = 1$. Fig. 8 is the results of the four methods. We can see that the "DLT" method is better than the "DLT2" method and the performance of the "Normalized" method is comparable to that of the "Normalized2" method. Hence different line parameterizations do have some influence on the results of the DLT method, but there has no noticeable influence on our normalized method.

4.2. Experiments with real image

In real image test, images are taken by a Nikon Coolpix 990 digital camera with the resolution of 1024×768. Fig. 9 shows two images of the test set, which are taken in our lab

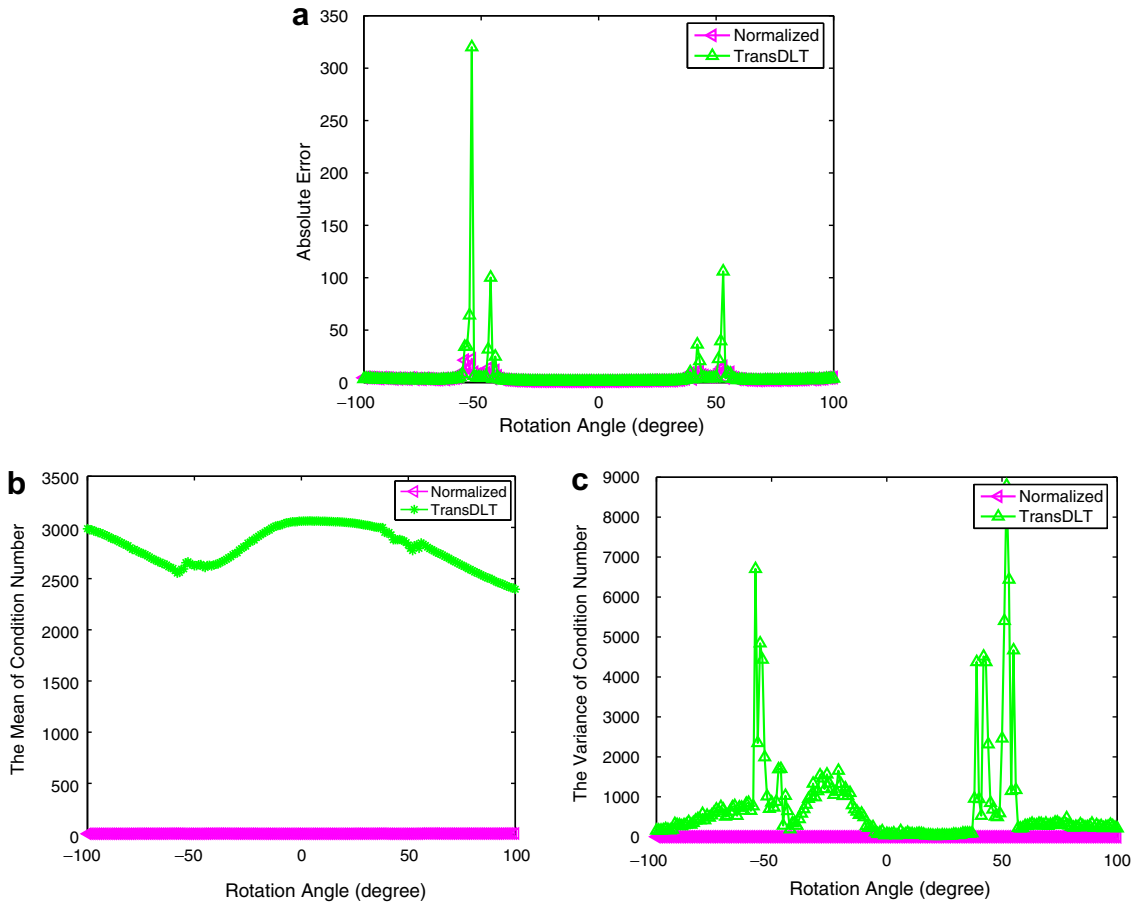

Fig. 7. A comparison of the "TransDLT" method and our normalized method.

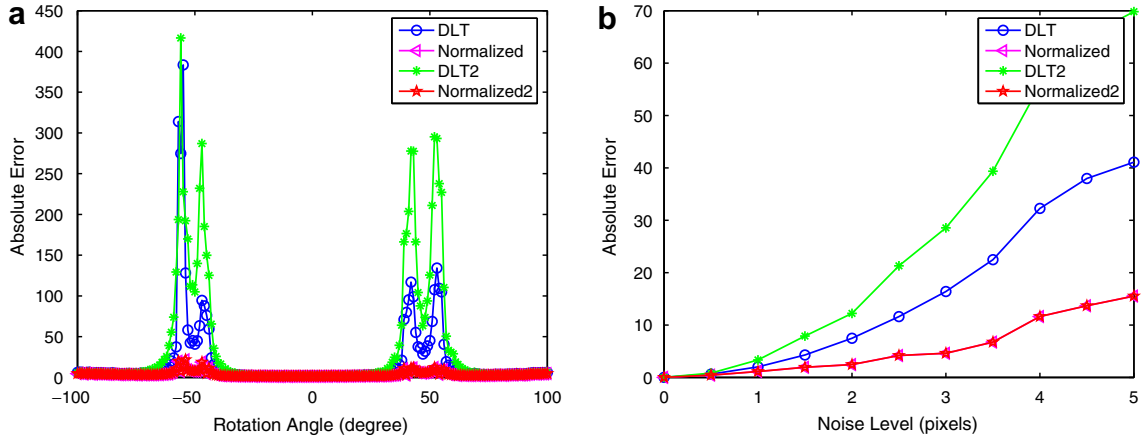

Fig. 8. A comparison of the measurement's absolute error of the four methods.

with the "⊡"-type reference template laid on the ground. Fig. 10 shows two images taken in a parking. During the test, we take the template lines as 3D space lines and their space coordinates are known. To obtain the corresponding image lines, we first use canny edge detector to detect the edge points. Then we use a least-squares technique to fit the detected edge points into lines. Finally, we use the DLT method and our normalized method to measure the distances on the ground. The comparative results are shown in Tables 1 and 2, where the true distances are taken manually on the spot. From the test results of Figs. 9a and 10a, we can see that the two methods are of comparable accuracy and the normalized method performs slightly better than the DLT method. From the test results of Figs. 9b and 10b, we can see that the accuracy of the normalized method is far better than the DLT method. The reason is

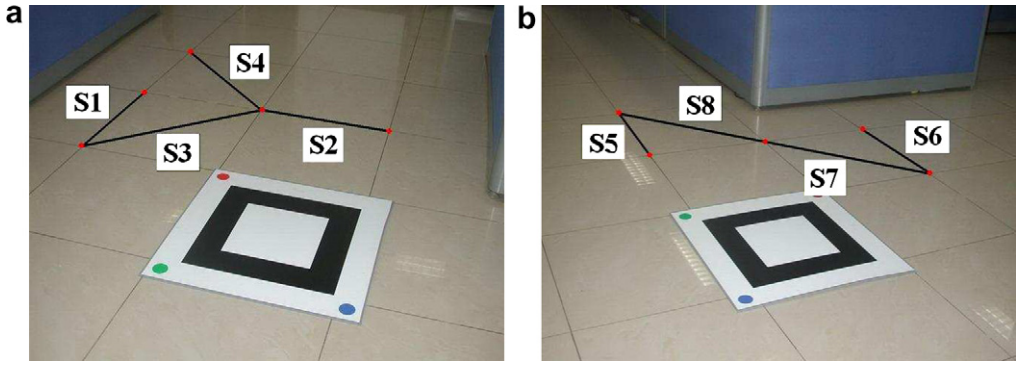

Fig. 9. Two test images taken in our lab.

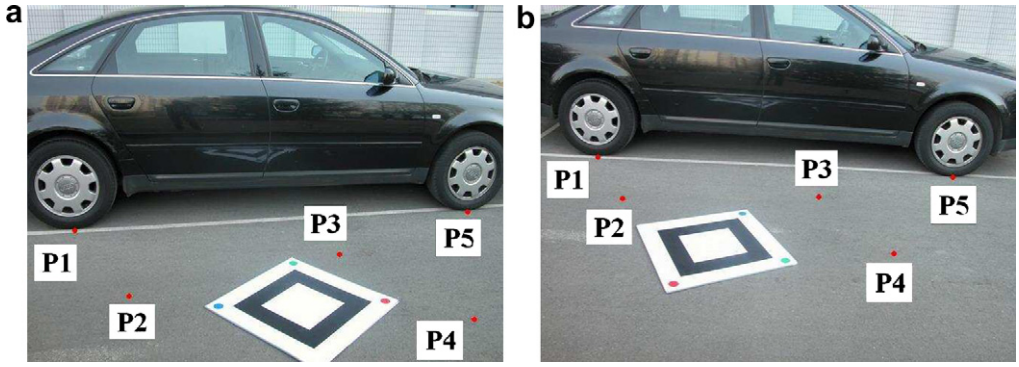

Fig. 10. Two test images taken in the parking.

Table 1
A comparison of the two methods with real images in Fig. 6

	Line segments							
	S_1	S_2	S_3	S_4	S_5	S_6	S_7	S_8
True distance (cm)	60	60	84.85	84.85	60	60	84.85	84.85
DLT method								
Estimated value (cm)	59.44	59.56	84.17	84.41	57.07	57.81	82.22	82.79
Absolute error (cm)	0.56	0.44	0.68	0.44	2.93	2.19	2.63	2.06
Relative error (%)	0.93	0.73	0.80	0.52	4.88	3.65	3.10	2.43
Normalized method								
Estimated value (cm)	59.71	59.80	84.31	84.50	59.66	59.41	84.82	84.17
Absolute error (cm)	0.29	0.20	0.54	0.35	0.34	0.59	0.03	0.68
Relative error (%)	0.48	0.33	0.64	0.41	0.57	0.98	0.04	0.80

Table 2
A comparison of the two methods with real images in Fig. 7

	Line segments							
	P_1P_2	P_2P_3	P_3P_4	P_4P_5	P_1P_2	P_2P_3	P_3P_4	P_4P_5
True distance (cm)	94	126.5	87.5	147.5	94	126.5	87.5	147.5
DLT method								
Estimated value (cm)	99.38	128.52	87.49	145.51	88.65	139.65	84.38	165.72
Absolute error (cm)	5.38	2.02	0.01	1.99	5.35	13.15	3.12	18.22
Relative error (%)	5.72	1.60	0.01	1.35	5.69	10.40	3.57	12.35
Normalized method								
Estimated value (cm)	96.48	127.95	87.09	146.02	90.86	130.41	86.35	152.21
Absolute error (cm)	2.48	1.45	0.41	1.48	3.14	3.91	1.15	4.71
Relative error (%)	2.64	1.15	0.47	1.00	3.34	3.09	1.31	3.19

that there exists at least one template line close to the origin of the image coordinate system in both Figs. 9b and 10b, and Figs. 9a and 10a do not contain such lines.

5. Conclusion

In this paper, we present a new normalized method for line-based homography estimation and apply it to visual metrology. Although the estimation based on line correspondences is considered as a dual of the one based on point correspondences, or is regarded projectively equivalent, we find from the numerical point of view, the estimation based on line correspondences has its own specialties, and these specialties must be accounted for robustness concern. For example, we find that if an image is close to the origin, the case is numerically a critical one. In addition, the Hartley's normalization seems to be designed for point bases estimation (in fact, unlike a pair of corresponding points, a pair of corresponding lines across two images does not give rise any constraints on fundamental matrix), it cannot be directly used for our line-based homography estimation. Simulations and real image tests show our proposed new normalization method can adequately remove the risky cases, and can significantly increase the measurement accuracy and robustness.

Acknowledgement

This work was supported by the National Key Basic Research and Development Program (973) under Grant No. 2002CB312104 and the National Natural Science Foundation of China under Grant No. 60633070.

References

Abdel-Aziz, Y., Karara, H., 1971. Direct linear transformation from comparator into object space coordinates in close-range photogrammetry. In: Proc. Symp. on Close-Range Photogrammetry, Urbaba, IL, pp. 1–18.

Agarwal, A., Jawahar, C.V., Narayanan, P.J., 2005. A Survey of Planar Homography Estimation Techniques. Technical Reports, International Institute of Information Technology, Hyderabad (Deemed University).

Criminisi, A., 2001. Accurate Visual Metrology from Single and Multiple Uncalibrated Images. Springer-Verlag Press.

Criminisi, A., Reid, I., Zisserman, A., 1999. Single view metrology. In: Proc. 7th IEEE Internat. Conf. on Computer Vision, pp. 434–441.

Faugeras, O., 1993. Three-dimensional Computer Vision: A Geometric Viewpoint. MIT Press.

Hartley, R., 1997. In defence of the eight-point algorithm. IEEE Trans. Pattern Anal. Machine Intell. 19 (6), 580–593.

Hartley, R., Zisserman, A., 2003. Multiple View Geometry in Computer Vision, second ed. Cambridge University Press.

Horn, R.A., Johnson, C.R., 1990. Matrix Analysis. Cambridge University Press (Reprint edition).

Kanatani, K., Ohta, N., 1999. Accuracy bounds and optimal computation of homography for imagemosaicing applications. In: Proc. 7th IEEE Internat. Conf. on Computer Vision, pp. 73–78.

Triggs, B., 1998. Autocalibration from planar scenes. In: Proc. 5th European Conf. on Computer Vision, pp. 89–105.

Wang, G.H., Hu, Z.Y., Wu, F.C., 2004. Single view measurement based on space planes. J. Comput. Sci. Technol. 19 (3), 374–382.

Wang, G.H., Tsui, H.T., Hu, Z.Y., Wu, F.C., 2005. Camera calibration and 3D reconstruction from a single view based on scene constraints. Image Vision Comput. 23 (3), 311–323.

Wright, J., Wagner, A., Rao, S., Ma, Y., 2006. Homography from coplanar ellipses with application to forensic blood splatter reconstruction. In: IEEE Comput. Soc. Conf. on Computer Vision and Pattern Recognition, pp. 1250–1257.

Zhang, Z., 2000. A flexible new technique for camera calibration. IEEE Trans. Pattern Anal. Machine Intell. 22 (11), 1330–1334.